Siegert-pseudostate representation of quantal time evolution: A harmonic oscillator kicked by periodic pulses

Seiichi Tanabe,[1] Shinichi Watanabe,[1] Naoki Sato,[1] Michio Matsuzawa,[1] Shuhei Yoshida,[2] Carlos Reinhold,[3] and Joachim Burgdörfer[2,3,4]

[1]*Department of Applied Physics and Chemistry, University of Electro-Communications, 1-5-1, Chofu-ga-oka, Chofu-shi, Tokyo 182-8585, Japan*

[2]*Institute for Theoretical Physics, Vienna University of Technology, Wiedner Hauptstrasse 8-10/136, A-1040 Vienna, Austria*

[3]*Oak Ridge National Laboratory, Post Office Box 2009, Oak Ridge, Tennessee 37831-6373*

[4]*Department of Physics and Astronomy, University of Tennessee, Knoxville, Tennessee 37996-1200*

(Received 16 October 2000; published 19 April 2001)

Finiteness of the computational resources is a hindrance to representing the time evolution of an infinitely extended system. Several numerical techniques are available for mimicking the nonboundedness of the system despite the restricted Hilbert space of the employed expansion basis set. We present a formulation based on the outgoing-wave Siegert pseudostates. A harmonic oscillator exposed to a periodic train of impulsive pulses (''kicks'') demonstrate the efficiency of the Siegert method.

DOI: 10.1103/PhysRevA.63.052721 PACS number(s): 32.80.Fb, 31.15.−p, 02.70.−c, 32.80.Rm

I. INTRODUCTION

Quantum calculations involving continuum states are hampered by the finiteness of the basis set intended to span the much bigger true solution space. The truncation needed for computer calculations then requires mimicking the correct behavior of the system beyond the finite boundary. Since the external solution is usually unknown, one is forced to adopt a reasonable substitute to model the correct physics of the system in the external region. Mismatch of solutions at the outer boundary causes reflection, which, in turn, produces interferences with the localized portion of the wave packet. The finite size of the basis space thus leads eventually to a catastrophic collapse of the evaluation of the S matrix. Aspects of reflectionless propagation have been discussed in Ref. [1] within the framework of pseudostate expansions. Unlike for grid-based finite-element or finite-difference methods, introduction of ''masking'' is complicated for pseudostate methods. We overcame the reflection of waves off the outer boundary of the Hilbert space using four alternative methods. The use of outgoing-wave basis functions was briefly presented as a promising procedure to achieve this goal [1]. We present in the following a more detailed account of the formulation of the time-propagation method based on this outgoing-wave basis set, widely known as the Siegert pseudostates (SPS) [2,3].

The quantum model system that we take up here is a radial harmonic oscillator subject to a train of periodic half-cycle pulses (HCPs for short) with the δ-function profile in time, a benign artifact readily modifiable to represent a given experimental profile. The time-dependent perturbation potential is given by

$$V(t,z) = -z\Delta p \sum_{k=1}^{N} \delta(t-kT),$$

where T is the period between successive pulses. Consideration of this problem has been motivated by both experimental [4] and theoretical [5] studies of ionization of Rydberg atoms by a train of HCPs. For simplicity, we limit ourselves in the following to a radial harmonic-oscillator potential. This simplified situation actually arises when we diagonalize the atom-field Hamiltonian adiabatically by regarding r, the electron's radial distance from the nucleus, as the adiabatic variable. Retaining either the highest up-field ($\Delta p<0$) or the lowest down-field ($\Delta p>0$) Stark potential, this procedure results in an effective potential energy operator that yields an effective one-dimensional (1D) representation of the atom-pulse system.

One goal of this paper is to understand the dynamical features of this model system in terms of the operationally defined ''survival'' probability against ionization. It may well be wondered how the survival probability may be meaningfully defined for a particle in a harmonic potential that, at face value, is nothing but a bound system. What we have in mind is a potential that is locally harmonic but becomes perfectly absorptive at some radial distance r_0. Classically, this situation is realized when the potential flattens out at the cutoff radius r_0, beyond which it is represented by a constant (Fig. 1). Quantum mechanically, such a sharp edge induces weak but genuine reflection. Representation of perfect absorption by such a truncated potential is only an approximation in quantum mechanics. In any case, an interesting realization of this model would be a magneto-optically trapped atom. We may denote by $P_N(n_0:n^*)$ the probability of the harmonic oscillator initially in state n_0 to remain in states below n^* after being exposed to a train of N impulsive pulses. The state n^* serves as the upper bound in energy, beyond which we presume the oscillator ''ionizes'' with no recovery of flux into lower states. With this definition of ''ionization,'' the survival probability against ionization is given by $P_N(n_0:n^*)$.

We note in passing that the excitation processes of a simple harmonic oscillator have a history of investigations under the title of a ''driven harmonic oscillator.'' Much is known about its analytical solutions [6], in the particular

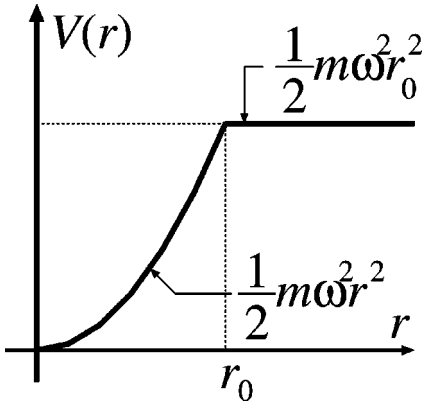

FIG. 1. Representation of the potential energy of the target oscillator corresponding to the absorptive boundary condition. It is perfectly absorptive in classical mechanics but allows weak reflection in quantum mechanics.

case of the sinusoidal driving fields. Such a driving field, however, imparts no net momentum on the average. In this regard, the present study may be in line with a recent one on periodic kicks of an oscillator by spatially modulated pulses [7] (see also [8]).

The paper is organized as follows. In Sec. II, the present model and its treatment are described, together with the somewhat unfamiliar concept of the Siegert pseudostates. Some mathematical details including the Siegert Green's functions for this section are relegated to Appendixes. Section III discusses the classical phase-space structure of this system, which aids in the interpretation of the quantum ''survival'' probability in Sec. IV. The determination of P_N demonstrates the use of the Siegert pseudostates for the present unbounded system. We also compare its efficiency with another reflection elimination scheme, the masking method for truncated pseudostate expansions.

II. MODEL AND FORMULATION

A. Description of the model

The Hamiltonian for the kicked radial 3D harmonic oscillator reads

$$H=-\frac{\hbar^2}{2m}\frac{\partial^2}{\partial r^2}+\tfrac{1}{2}m\omega^2 r^2-r\Delta p\sum_{k=1}^{N}\delta(t-kT), \qquad (1)$$

where the first two terms represent the Hamiltonian H_0 of the radial degree of freedom of the unperturbed 3D harmonic oscillator and the last term represents the interaction Hamiltonian $V(t)$ for the train of electromagnetic pulses to the atom. The radial wave function must vanish at the origin $r=0$. Here, Δp is the momentum transfer and T is the period between kicks. Equation (1) can be derived from a diagonalization of the atom-field Hamiltonian when r is treated as the adiabatic variable [9]. This modeling of $V(t)$ amounts to taking the highest ($\Delta p<0$) or the lowest ($\Delta p>0$) of the eigenvalues of $\cos\theta$ at a fixed value of r. In a real three-dimensional situation, they will appear simultaneously with the other intermediate roots of $\cos\theta$. The δ-function representation of each kick amounts, of course, to assuming that the pulse duration is short in comparison to the period of the oscillator.

Because of the particularly simple dependence of the kicks on time, the time integral of the interaction term is characterized only by the momentum transfer. We thus have the time propagator per kick period as

$$U(0,T)=e^{ir\Delta p/\hbar}e^{-iH_0T/\hbar}. \qquad (2)$$

This is exact for the present δ-function representation of the interaction Hamiltonian. The train of N kicks is represented by

$$U^N(0,T)=[e^{ir\Delta p/\hbar}e^{-iH_0T/\hbar}]^N. \qquad (3)$$

The exponentiation of the coordinate operator is facilitated by the use of the discrete-variable representation (DVR) basis set [10]. To be specific, we construct a set of coordinate space basis functions $\{\pi_i(r)\}$, starting with a set of Legendre polynomials and the associated Gaussian quadrature rule, such that

$$\pi_i(r_j)=0 \quad \text{unless} \quad i=j. \qquad (4)$$

In accordance with the prescription in Appendix B, we have

$$\int \pi_i(r)e^{ir\Delta p/\hbar}\pi_j(r)dr\simeq e^{ir_j\Delta p/\hbar}\delta_{ij}. \qquad (5)$$

Note that the restriction of the configuration space to within $r\leqslant r_0$ means that the action of the field is also suppressed outside this range. However, the field outside generally continues to accelerate the particle outward so that the survival probability is unlikely to be affected by the neglected exterior region by our projection method. (This expectation holds rigorously in classical mechanics.) For the purpose of examining our model problem, we will consistently suppress the exterior effect of kicks hereafter.

B. Construction of Siegert pseudostates (SPS)

Here we wish to summarize essential facts about the reflectionless propagation by the Siegert pseudostates. Technical details related to the Siegert-pseudostate representation of the Green's function and its associated time propagator are discussed in Appendixes A and C.

The Siegert boundary condition is an explicit imposition of the outgoing or incoming wave condition on a sphere with radius $r=r_0$ dividing the inner and outer region,

$$\left(\frac{d}{dr}-ik\right)\psi(r)\big|_{r=r_0}=0. \qquad (6)$$

Here and in the following, the function $\psi(r)$ is a radial wave function, i.e., it is premultiplied by r, which is consistent with the factor $\xi(r)$ for $\phi(r)$ of Appendix B so that the term $1/r$ of Ref. [2] is absent in our case. Remarkably, the solutions to the Schrödinger equation subject to this boundary condition can be obtained by solving a single complex eigenvalue problem [2] resulting in a spectral representation of the

Green's function with complex-valued eigenenergies. Indeed, the advanced Green's function is found to be

$$G^{(-)}=\sum_{n=1}^{N}\frac{c^{(n)}c^{(n)T}}{E_n-E}\quad(\mathrm{Im}E_n<0),\tag{7}$$

as discussed in Appendix C. This means, upon Laplace transform, that the time propagation of the Siegert pseudostates is simply represented by the factor

$$e^{-iE_nt/\hbar}\quad(\mathrm{Im}E_n<0)\tag{8}$$

for each Siegert state.

C. Passage between SPS and DVR

The DVR is an orthonormal basis set in the standard sense but the orthonormality of the Siegert pseudostates is defined differently. This requires knowledge of the somewhat nontrivial SPS-to-DVR transformation.

We may expand a Siegert state as

$$\psi_n(r)=\sum_i c_i^{(n)}\pi_i(r).\tag{9}$$

Consider the inverse problem of representing $\pi_i(r)$ in terms of the Siegert pseudobasis $\{\psi_n(r)\}$, namely

$$\pi_i(r)=\sum_n b_i^{(n)}\psi_n(r).\tag{10}$$

This leads to the identity

$$\pi_i(r)=\sum_{n,j} c_i^{(n)}b_j^{(n)}\pi_j(r)\tag{11}$$

demanding

$$\delta_{ij}=\sum_n c_i^{(n)}b_j^{(n)}.\tag{12}$$

Thus the matrices $b_j^{(n)}$ and $c_i^{(n)}$ are mutually inverse, namely, they represent linear transformation of basis sets in the standard sense of linear algebra. High roots of the Siegert eigenvalue problem are numerically unsatisfactory and cause flaws in time propagation if retained. This difficulty is circumvented by first dropping a certain number of high roots. The inverse of the resulting *rectangular* matrix may be obtained by application of the singular-value decomposition procedure documented in standard textbooks on numerical methods [11].

For notational convenience, let us write

$$\langle\psi_n|\pi_i\rangle=c_i^{(n)},\tag{13}$$

$$\langle\pi_i|\psi_n\rangle=b_i^{(n)}\tag{14}$$

with the understanding that the bra-ket notation here means strictly the transformation from Siegert states to DVR or its inverse with the requirement that the transformation matrices are rectangular rather than square. Then the following holds in the standard manner:

$$\langle\pi_i|\pi_j\rangle=\delta_{ij},\tag{15}$$

$$\sum_i|\pi_i\rangle\langle\pi_i|=\mathbf{1}.\tag{16}$$

With this notation, we may write the time propagator between kicks with respect to the Siegert pseudostates as

$$U_{m,n}(0,T)=\sum_i\langle\psi_m|\pi_i\rangle\times\langle\pi_i|\exp(r_i\Delta p)|\pi_i\rangle\langle\pi_i|\psi_n\rangle\times\exp(-E_nT).\tag{17}$$

D. Treatment by masking method

In reducing the unphysical reflection, the masking method has the merit of relying only on real algorithms and of being easy to use. The method multiplies the wave packet $\Psi(t,r)$ by the profile function $f_p(r)(\geqslant 0)$ at some appropriate time interval Δt. The profile function is effective at some $r>r_{\mathrm{mask}}$ such that

$$f_p(r)\begin{cases}=1 & (r<r_{\mathrm{mask}})\\ <1 & (r>r_{\mathrm{mask}}).\end{cases}\tag{18}$$

Almost any functional form meeting this condition works, for instance,

$$f_p(r)=\cos\left(\frac{\pi}{2}\left[\frac{r-r_{\mathrm{mask}}}{r_{\mathrm{max}}-r_{\mathrm{mask}}}\right]\right)\quad(r>r_{\mathrm{mask}}),$$

where $r_{\mathrm{max}}\geqslant r_{\mathrm{mask}}\geqslant r_0$ indicates the outer boundary for masking.

If the masking interval Δt is too coarse, reflection is insufficiently reduced, resulting in a poorly converged S matrix. If it is too fine, it causes a strong reflection as discussed in Ref. [1] in the context of the quantum Zeno effect. There exists some optimal choice of Δt found by trial and error. The prescription of the method is straightforward for merely suppressing the reflection. Given the wave packet $\Psi_{\mathrm{before}}(t,r)$ at time t,

$$\Psi_{\mathrm{after}}(t^+,r)=f_p(r)\Psi_{\mathrm{before}}(t,r)\tag{19}$$

for t^+ infinitesimally greater than t.

For basis expansion methods, unlike for grid-based discretization techniques, imposing a mask is more involved here. We consider the following implementation of the masking approximation. First, applying the masking immediately at the border $r=r_0$ introduces uncertainty in the definition of the border itself. We consider the auxiliary problem for which the potential is extended beyond r_0, namely

$$V(r)=\tfrac{1}{2}m\omega^2r^2\quad(r<r_0)$$

$$=\frac{1}{2}m\omega^2 r_0^2 \quad (r_0<r<r_{\max}). \tag{20}$$

As noted in the Introduction, this potential is intended to mimic absorption, if approximate, in quantum mechanics. To make the effect of the kicks in the Siegert and masking method identical in the exterior region, the kick is set to act on this model system only in the range $r<r_0$.

With this understanding, we solve the stationary states for this model using the trigonometric basis set $\{\eta_n(r)\}$ defined by

$$\eta_n(r)=\sqrt{\frac{2}{r_{\max}}}\sin\left(\frac{n\pi}{r_{\max}}r\right). \tag{21}$$

This basis set is convenient because the Hamiltonian can be evaluated analytically, even though it is appallingly slow in convergence, as will be seen later. Likewise, the matrix elements of r in the range $r<r_{\max}$ as well as the matrix elements of the profile function f_p are expressible analytically. Thus, the action of the profile function on the wave packet is representable by a mere matrix multiplication on the basis set $\{\eta_n(r)\}$.

III. CLASSICAL MECHANICS OF THE MODEL PROBLEM

The classical dynamics of this model system may provide useful insights into the ''ionization'' dynamics and, thereby, shed light on quantum dynamics. The correspondence between classical and quantum dynamics is expected to be as close in this system as for harmonic systems because classical and quantum expectation values should agree, according to Ehrenfest's theorem. Clearly, in the present case the correspondence can only be approximate due to the anharmonic cutoff of the potential at r_0.

The equations of motions can be converted into a discrete map connecting phase-space coordinates of adjacent kicks,

$$r_n^+=r_n^-, \tag{22}$$

$$p_n^+=p_n^-+\Delta p, \tag{23}$$

$$r_{n+1}^-=\left|r_n^+\cos\omega T+\frac{p_n^+}{m\omega}\sin\omega T\right|\equiv|a_n|, \tag{24}$$

$$p_{n+1}^-=\frac{a_n}{|a_n|}(p_n^+\cos\omega T-r_n^+ m\omega\sin\omega T). \tag{25}$$

In Eqs. (22)–(25), the superscript $\pm$ stands for the infinitesimal time increments $\pm\varepsilon$ just after $(+)$ or before $(-)$ the nth kick. The kick period is denoted by T and the oscillator frequency by ω. The corresponding oscillator period is denoted by T_ω. During the interval in between kicks $[nT+\varepsilon,(n+1)T-\varepsilon]$, the energy of the oscillator,

$$E_n=\frac{p_n^2}{2m}+\tfrac{1}{2}m\omega^2 r_n^2, \tag{26}$$

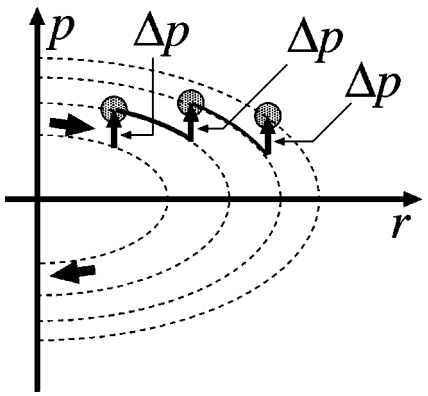

FIG. 2. Graphical representation as to how the oscillator hops from one ellipse to another upon receiving a kick. It may as well occur that a subsequent kick is received after several revolutions on a particular ellipse.

remains constant so that the trajectory travels on an ellipse in phase space. One catch, however, is that for a 3D harmonic oscillator, the condition $r\geqslant 0$ must be satisfied. Only half of the ellipse is accessible and the period is given by $T_\omega=\pi/\omega$. Figure 2 graphically illustrates how each kick affects the oscillator's trajectory in phase space. The trajectory revolves on the half-ellipse until the next kick shoves it onto another half-ellipse. In the present case, we consider positive kicks, $\Delta p>0$, pushing the electron radially outward. This process continues until the trajectory reaches beyond the half-ellipse that marks the threshold for ionization. More detailed insights into the classical phase-space structure can be extracted from a Poincaré surface of section (Fig. 3). The phase space is covered by concentric elliptically shaped tori up to a critical torus where the turning point touches the transition point r_0 to the ''continuum.'' Outside the critical

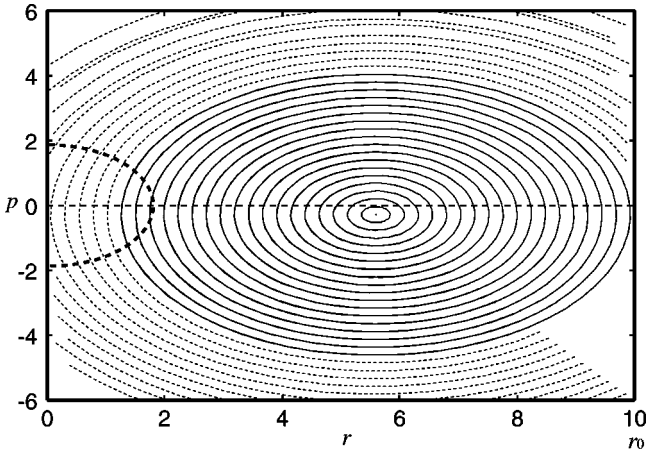

FIG. 3. Poincaré surface of sections representing stroboscopic snapshots (r_n^-,p_n^-) of an ensemble of trajectories (Table I), taken just prior to the kicks. The initial conditions are such that the trajectories are positioned along the line joining the unique center of the ellipses and the lower right corner of the figure with an equal spacing. The dashed ellipses ''ionize'' whereas the solid ones remain bound. The thick dashed line corresponds to the energy constant manifold with $E=3/2\hbar\omega$.

torus, the propagation on the ellipse is of finite duration. As soon as the phase point reaches the half-space $r>r_0$ for the first time, the motion on the torus is truncated and the trajectory is lost. All concentric ellipses are centered about

$$r_{\text{center}}=\frac{\Delta p}{m\omega^2 T}, \quad p_{\text{center}}=-\frac{\Delta p}{2}. \tag{27}$$

The position of the center can be easily understood in terms of a ''Stark-shifted'' oscillator. In the case in which several kicks occur during one orbital period ($T<T_\omega$), the time average over the perturbation can be represented by a Stark field $F=\Delta p/T$,

$$\langle V\rangle=-r\frac{\Delta p}{T}. \tag{28}$$

The displaced harmonic oscillator is thus described by the effective Hamiltonian

$$H_{\text{eff}}=\frac{(p-p_{\text{center}})^2}{2\,m}+\tfrac{1}{2}m\omega^2(r-r_{\text{center}})^2. \tag{29}$$

Comparison between Eqs. (28) and (29) yields the condition for r_{center} [Eq. (27)]. Likewise, the condition that the kicks preserve the kinetic energy

$$p\Delta p+\frac{\Delta p^2}{2}=0 \tag{30}$$

defines the symmetry axis in the p direction with $p_{\text{center}}=-\Delta p/2$ for the momentum just prior to the kick. We note in passing that highly nontrivial phase-space structures emerge when the center of ellipse r_{center} is closer to the origin than to r_0, i.e., $r_{\text{center}}<r_0/2$. Because the map is discontinuous at the origin, the elliptic tori are destroyed. In particular, in the case of classical resonances, i.e., the kick period T is such that

$$T\simeq\frac{k\pi}{n\omega}, \tag{31}$$

where k and n are integers and mutually prime, that is, the fraction k/n is irreducible, some phase-space trajectories travel on an Arnold web [8] whose rich structure and implication for the quantum dynamics is currently under investigation and will be presented elsewhere [12].

The classical phase-space portrait immediately allows us to determine the classical survival of an initial state for which we take in the following the ground state of the field-free harmonic oscillator. In general, the initial bundle of trajectories traveling on off-centered ellipses either all reach beyond r_0 or all fail to reach r_0. Under a particular circumstance (to be specified below), only a fraction of the trajectories reach r_0 resulting in ionization while leaving behind the residual trajectories within the ionization boundary. The survival probability in this event differs from both zero and unity.

The region of survival is delimited by two tori as upper and lower bounds that meet the following conditions: (i) they both touch the boundary at $r=r_0$, (ii) one of them touches at $r=0$ the maximum (classical) momentum of the initial field-free torus $p=\sqrt{3\hbar\omega m}$ (for the ground state), and (iii) the other touches the maximum elongation in coordinate space $r_1=\sqrt{\hbar/m\omega}$ at $p\approx 0$. This range of ellipses can be converted into a range of kick periods, T, for which the classical survival probability varies between zero and one at fixed kick strength Δp and oscillator frequency ω,

$$\frac{2\Delta p}{m\omega^2}\frac{1}{r_0+r_1}<T<\frac{2\Delta p}{m\omega^2}\frac{r_0}{r_0^2-r_1^2}. \tag{32}$$

TABLE I. Parameters for the kicked harmonic oscillator as used for numerical implementations.

Definition	Value
Oscillator's mass	$m=1$
Oscillator's angular frequency	$\omega=1$
Initial-state quantum number	$n=1$
Boundary distance	$r_0=10$
Momentum transfer	$\Delta p=0.56$
Kick time interval	$T=0.1$

IV. NUMERICAL DEMONSTRATION

We first examine the convergence of the Siegert pseudostate method. We focus in the following on the case of positive Δp, that is, the so-called downhill case. Since ionization for the uphill case $\Delta p<0$ should involve angular degrees of freedom, coupling to other eigenstates of $\cos\theta$ would be required for a realistic representation. We set the parameters as shown in Table I. At the given values of Δp and T, the survival probability and, likewise, the ionization probability maintain a finite value differing noticeably from both zero and unity even after over 100 kicks [see Eq. (32)]. These probabilities may be affected by the occurrence of reflections, which limits the reliability of the quantal calculation. The basis size for the Siegert method is set to 200, although convergence can be attained even with a slightly smaller basis set. This specification is all we need for this method. For the masking method, the time interval Δt of masking is such that we apply it ten times during T, $T=10\Delta t$, and r_{mask} is set to 25 and $r_{\max}=30$, i.e., the absorbing layer is situated between 25 and 30 a.u. The number of basis functions is varied from 500 to 2000 for comparison. A rather large number of basis functions are needed to represent a sharp potential edge at r_0 on account of the rather naive choice of the trigonometric basis set.

Figure 4 shows the survival probability after each kick as a function of time t measured for the particular parameter set of Table I, where the discrepancy between the masking method and the Siegert method becomes more pronounced with increasing time. The results with the masking method approach that of the Siegert pseudostate method as the basis size increases, even though it does so remarkably slowly. Each bump in Fig. 4 occurs when the wave packet starting originally from the ground state of the field-free Hamiltonian

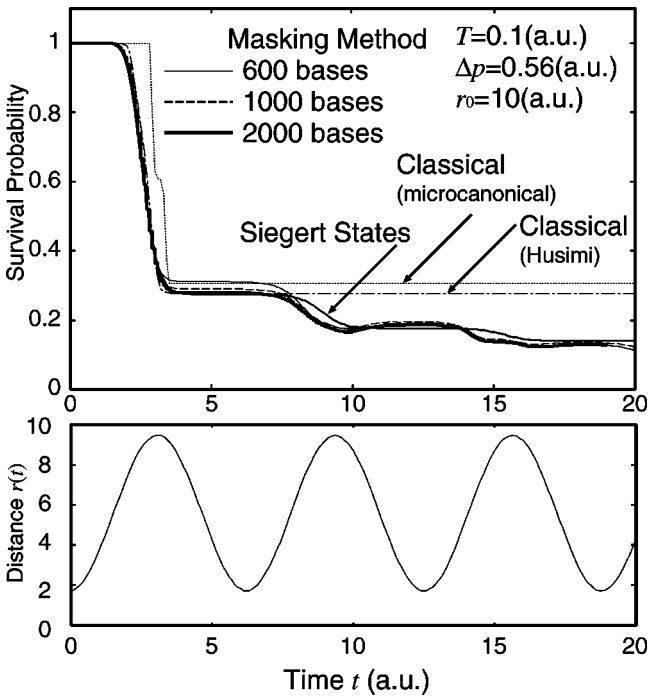

FIG. 4. Survival probability $P_N(1{:}50)$ after each kick as a function of time *t*. The solid line of a moderate thickness is for the Siegert method. The thin solid line, the broken line, and the thick solid line are for the masking method with 600, 1000, and 2000 basis functions, respectively. The slow convergence of the latter method is presumably due to the trigonometric basis functions. The dotted line represents the result of classical trajectory calculations using the microcanonical ensemble for initial trajectories, while the chain line uses the Husimi distribution of the initial-state wave function for generating initial trajectories. Plotted in the lower frame is the time evolution of radial distance *r* of a typical classical trajectory.

revisits the region near r_0. The classical survival probabilities, superimposed on Fig. 4, display only one drop-off followed by a stable plateau. For the classical calculation, we have employed two different initial ensembles, the standard microcanonical ensemble $P(r,p) \propto \delta(E-H_0(r,p))$, represented by the initial torus centered at the origin in Fig. 3, and the Husimi probability distribution $P(r,p)=1/2\pi(r^2+p^2)e^{-(r^2+p^2)/2}$ corresponding to the initial-state wave function $\propto H_1(r)e^{-r^2/2}$. The small discrepancy between the two classical results reflects the influence of the initial quantum ground state on the survival probability. The ground state, dominated by the zero-point fluctuations, is the most nonclassical state. In the limit of high quantum numbers, the two classical curves would coincide. The stability of the classical survival probability is not unexpected because the classical motion of the harmonic oscillator, while off-centered, involves no spreading in phase space. By contrast, the quantum wave packet broadens as it continues its travel in phase space. The flux loss thus recurs at each visit to the boundary. The area *A* of the torus representing the initial state (Fig. 3) gives the size of the quantum uncertainty, i.e., the size of the quantum unit cell, $A \approx h$. It is the size of this spread that allows additional ionization each time the quantum wave packet approaches r_0.

Snapshots of the wave-packet propagation at different times (or number of kicks) are shown in Fig. 5. The upper of each panel shows the Husimi distribution in relief plot and the lower in contour plot. The axes are radius *r* and momentum *p*. Notice how a part of the wave packet in the masking method gets reflected owing to the sharp edge and tends to travel ahead of the wave packet described by Siegert pseudostates. Notice also how a portion of the wave packet of the masking method gets transmitted into the exterior region separated from the residue and the reflected wave. This can also be observed in the survival probability shown in Fig. 4. The difference between the two quantum survival probabilities is marked in particular by the sagging of the masking method at each dropoff. Overall, however, the position of the center of gravity remains quite close during the first ≈ 100 kicks.

Figure 6 shows the survival probability as a function of the kick period *T*. As noted in Sec. III [Eq. (31)], resonances occur as a function of *T*. The size of the off-centered ellipses increases as *T* approaches a resonance and attains infinity at the resonance. As *T* moves away from the resonance, the ellipse shrinks, eventually falling well within the boundary located at $r_0=10$. On the basis of the classical dynamics, one readily deduces the following estimate for the temporal width of the resonance:

$$\Gamma_t \simeq \frac{2\Delta p}{m\omega^2}\frac{r_0}{r_0^2-r_1^2}, \tag{33}$$

where $r_1 \simeq \sqrt{\hbar/m\omega}$ as before. The width may also be defined visually as the area of each depletion dip near a resonance in Fig. 6 where the survival probability is significantly lower than unity. Figure 7 compares this classical formula to the quantum mechanically evaluated temporal width indicating good agreement.

V. SUMMARY

The Siegert pseudostate method has been shown to be an effective scheme for propagating wave packets in an open quantum system. Reflections are perfectly suppressed without any significant distortion of the wave packet near the boundary. By comparison with a trigonometric basis expansion and masking, we found the convergence of the Siegert method to be remarkably fast. Application to the radial harmonic oscillator with a cutoff displayed a limited classical-quantum correspondence. The classical phase-space analysis aids in the interpretation of the quantum survival probability but noticeable discrepancies appear, mainly due to the fact that the initial ground state is highly nonclassical. Further application to the problem of Arnold diffusion in ''weak chaos'' [8] is envisioned.

ACKNOWLEDGMENTS

This work was supported in part by a Grant-in-Aid for Exploratory Research, Ministry of Education, Science and Culture, Japan, by the NSF, the DCS, OBES, U. S. DOE,

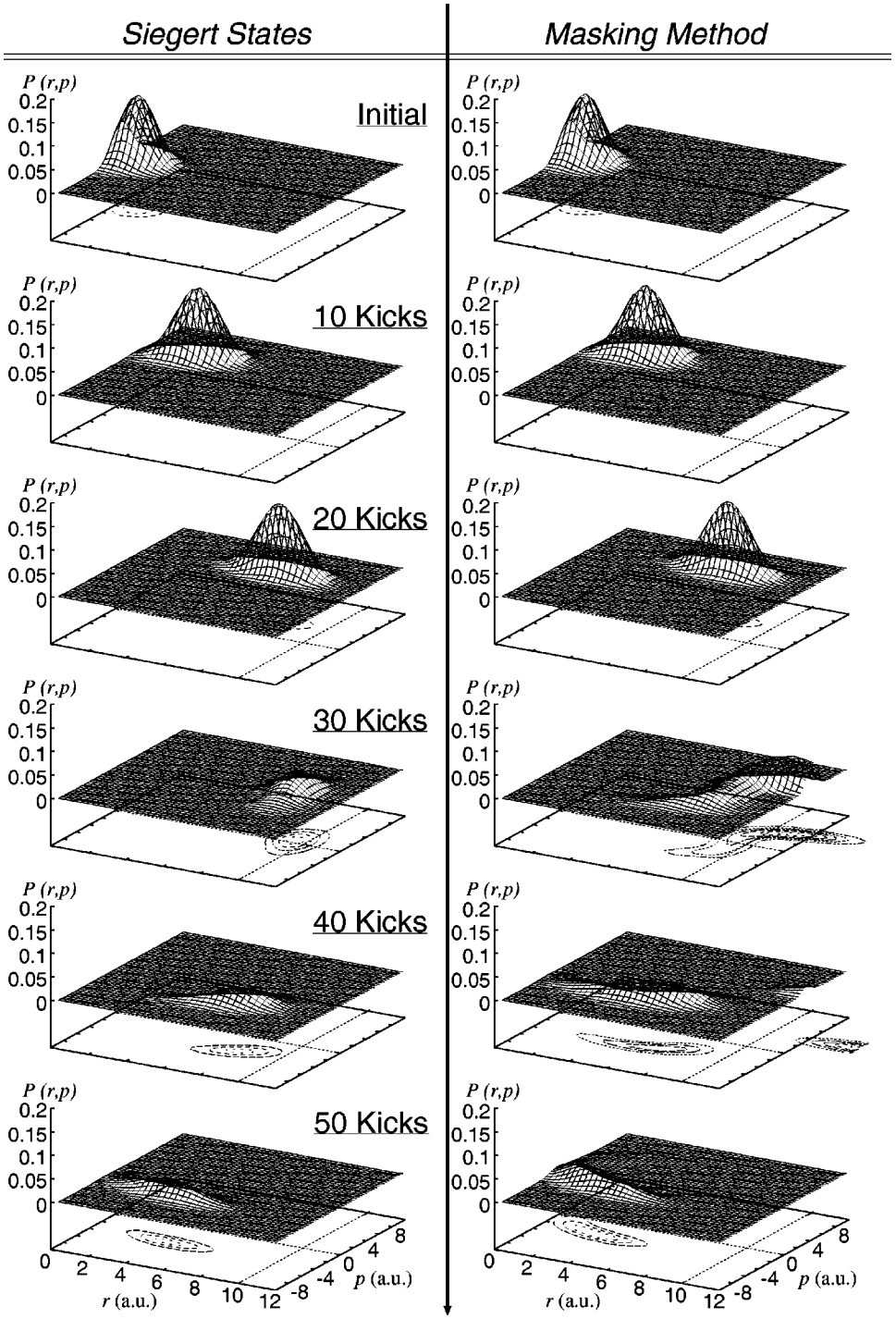

FIG. 5. Comparison of Siegert and masked wave packets using the Husimi distribution. Both relief and contour plots are shown for the indicated instances of kick. Differences arise due to the reflection incurred by the model potential for the latter method, particularly near $r=r_0$, where the harmonic potential is abruptly truncated. The masked wave packet tends to advance slightly. Note the change in vertical scale in relief plots as time elapses.

managed by UT-Battelle, LLC, under Contract No. DE-AC05-00OR22725, and the FWF-SFB016.

APPENDIX A: CONSTRUCTION OF SIEGERT PSEUDOSTATES

We work with the Hamiltonian multiplied by r_0^2, employing the Bloch operator to impose the Siegert boundary condition on the right-hand edge. Construction of the basis set in terms of DVR is described in Appendix B. The integrations are carried out over $x=(2r/r_0)-1$ from -1 to $+1$ to obtain various matrix elements. The eigensystem then reads

$$\sum_j (2\tilde{\mathcal{H}}_{ij}-\kappa\tilde{\mathcal{B}}_{ij}+\kappa^2\tilde{\mathcal{C}}_{ij})\tilde{c}_j=0,$$

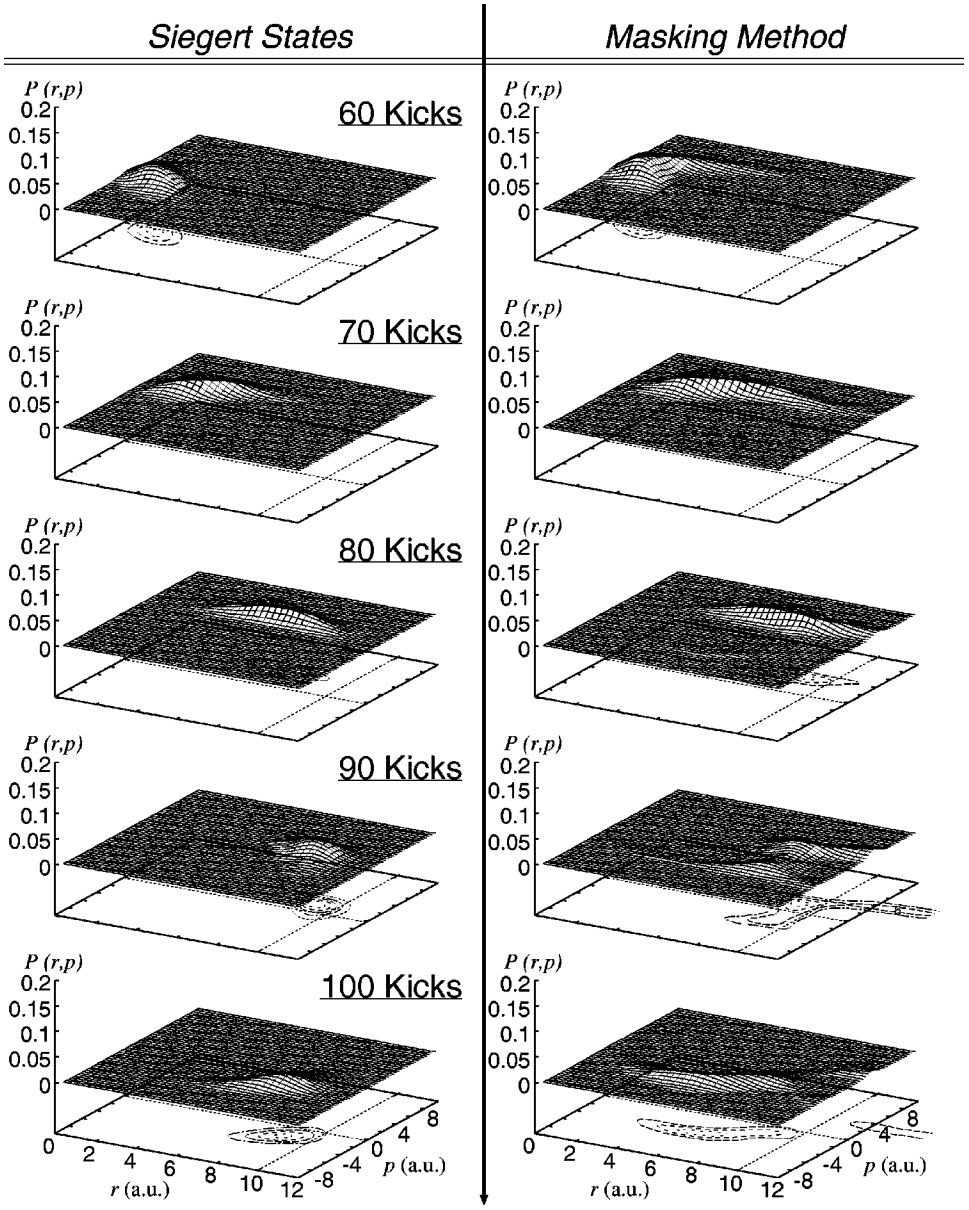

FIG. 5 (*Continued*).

where

$$\tilde{\mathcal{H}}_{ij} = -\tfrac{1}{2}\int_{-1}^{1} \psi_i'(x)\psi_j'(x)dx + r_0^2 \int_{-1}^{1} \psi_i(x)V(x)\psi_j(x)dx,$$

$$\tilde{\mathcal{B}}_{ij} = \psi_i(+1)\psi_j(+1),$$

$$\tilde{\mathcal{C}}_{ij} = r_0^2 \int_{-1}^{1} \psi_i(x)\psi_j(x)dx.$$

Here $\psi_i(x) = \xi(x)\pi_i(x)$ with the multiplier function $\xi(x)$ of Eq. (B2), and $V(x)$ pertains to the atomic potential that determines the target atom. The value of $\tilde{\mathcal{H}}_{ij}$ can be evaluated with Eq. (B1). Defining $c_j = [r_0\xi(x_j)]\tilde{c}_j$, we get

$$\mathcal{C}_{ij} = r_0^{-2}\xi(x_i)^{-1}\tilde{\mathcal{C}}_{ij}\xi(x_j)^{-1} = \delta_{ij}$$

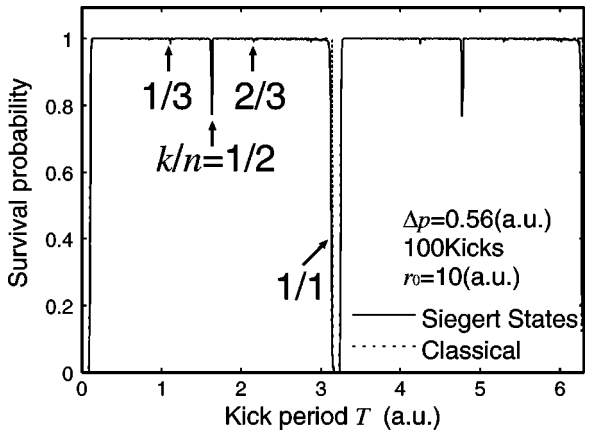

FIG. 6. Survival probability as a function of kick period T. Note the occurrence of 1/2, 1/3, and 2/3 resonances in addition to 1/1 resonance.

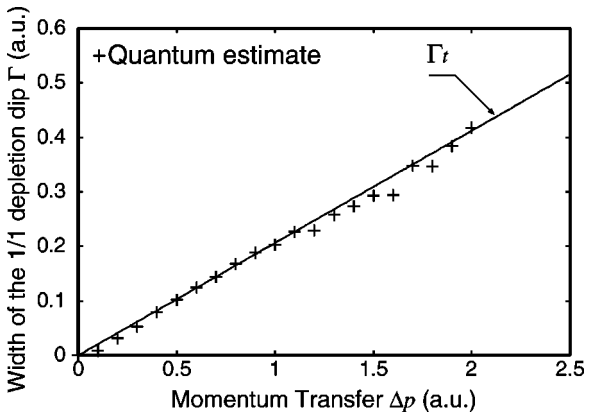

FIG. 7. Evolution of the width of the 1/1 depletion dip as a function of Δp. The solid line shows the estimate by classical mechanics as described in the text. The crosses show the widths numerically obtained on the basis of the visual gap in the survival probability curve.

so that we deal with orthonormalized basis functions of the standard type. With this redefinition of the coefficient vector,

$$\mathcal{H}_{ij}=r_0^{-2}\xi(x_i)^{-1}\tilde{\mathcal{H}}_{ij}\xi(x_j)^{-1},$$

$$\mathcal{B}_{ij}=r_0^{-2}\xi(x_i)^{-1}\tilde{\mathcal{B}}_{ij}\xi(x_j)^{-1}.$$

The eigensystem now reads

$$\sum_j (2\mathcal{H}_{ij}-\kappa\mathcal{B}_{ij}+\kappa^2\delta_{ij})c_j=0.$$

The above is equivalent to a linear system

$$\begin{pmatrix} 2\mathcal{H} & 0 \\ 0 & -\mathbf{1} \end{pmatrix}\begin{pmatrix} c \\ \kappa c \end{pmatrix}=\kappa\begin{pmatrix} \mathcal{B} & -\mathbf{1} \\ -\mathbf{1} & 0 \end{pmatrix}\begin{pmatrix} c \\ \kappa c \end{pmatrix}.$$

Let us rewrite this equation as

$$\mathcal{K}S_n=\kappa_n\rho S_n,$$

where

$$\mathcal{K}=\begin{pmatrix} 2\mathcal{H} & 0 \\ 0 & -\mathbf{1} \end{pmatrix},$$

$$\rho=\begin{pmatrix} \mathcal{B} & -\mathbf{1} \\ -\mathbf{1} & 0 \end{pmatrix},$$

in matrix notation, and

$$S_n=\begin{pmatrix} c_n \\ \kappa_n c_n \end{pmatrix}.$$

The matrices $\mathcal{H}$, $\mathcal{B}$, and $\mathbf{1}$ being real, it holds that if κ_n is an eigenvalue, so is κ_n^*, and likewise for the corresponding eigenvectors S_n and S_n^*.

One possible and practically straightforward normalization is then

$$S_m^T\rho S_n=c^{(m)T}\mathcal{B}c^{(n)}-(\kappa_m+\kappa_n)c^{(m)T}c^{(n)}$$

$$=-2\kappa_m\delta_{mn}. \tag{A1}$$

Completeness thus reads

$$\sum_{n=1}^{2N}\frac{1}{2\kappa_n}S_nS_n^T=\begin{pmatrix} 0 & \mathbf{1} \\ \mathbf{1} & -\mathcal{B} \end{pmatrix}.$$

Note the summation runs over all the $2N$ roots [2]. Attention must be paid to the expressions for physical quantities so that no explicit dependence on the normalization will appear as in the particular case of the Green's function in Appendix C.

APPENDIX B: APPROXIMATE EVALUATION OF MATRIX ELEMENTS

Equipped with the Gaussian quadrature associated with a selected orthogonal system of functions, the discrete variable representation (DVR) method [10] realizes a discretized spatial representation of the coordinate space. Obviously, classical polynomials are the first candidate for the orthogonal system because of the precise knowledge of their various integrals and of the celebrated Christoffel-Darboux formula, which yields an explicit transformation to DVR. Other choices of basis functions are possible and have been explored by other authors [13,14].

To set up the Siegert eigenvalue problem, we exploit the DVR method for approximately evaluating the matrix elements of differential operators. It must be noted, though, that a formally exact evaluation of various matrix elements is possible and is contained in an appendix of the paper by Tolstikhin *et al.* [2].

For the purpose of constructing Siegert pseudostates, the Legendre polynomials are a natural choice for basis set since they give a meaningful matrix representation of the Bloch operator. In accordance with Ref. [2], we define the normalized basis set $\{\phi_n(x)\}$,

$$\phi_n(x)=\sqrt{\frac{1}{h_{n-1}}}P_{n-1}(x) \quad (n=1,2,\ldots,N),$$

where h_{n-1} is the normalization constant. Upon discretization, the coordinate x becomes represented in terms of the Gaussian grid points $\{x_i\}$, namely the roots of $P_N(x)=0$, where $i=1,2,\ldots,N$. The associated DVR basis functions $\{\pi_i(x)\}$ are smooth over the interval $[-1,1]$ and satisfy

$$\pi_i(x_j)=\sqrt{\frac{1}{W_i}}\delta_{ij},$$

where W_i is the Gaussian-quadrature weight associated with $P_N(x)$. The DVR basis function $\pi_i(x)$ is merely a properly normalized Lagrange multiplier function,

$$\pi_i(x)=\sqrt{\frac{1}{W_i}}\prod_{j\neq i}\frac{(x-x_j)}{(x_i-x_j)},$$

but its practicality is far-reaching. The explicit transformation matrix between $\{\pi_i(x)\}$ and $\{\phi_n(x)\}$ derives from the Christoffel-Darboux formula, namely Eq. (C9) of Ref. [2],

$$\phi_n(x)=\sum_{i=1}^{N} T_{ni}\pi_i(x),$$

$$\pi_i(x)=\sum_{n=1}^{N} T_{ni}\phi_n(x),$$

where T_{ni}, an orthogonal matrix, readily proves to be $\sqrt{W_i}\phi_n(x_i)$.

Let us first recall that the matrix of an operator that does not involve derivatives is diagonal in DVR,

$$\int_{-1}^{1}\pi_i(x)g(x)\pi_j(x)dx\simeq\sum_k W_k\sqrt{\frac{1}{W_i}}\delta_{ik}\sqrt{\frac{1}{W_j}}\delta_{jk}g(x_k)$$

$$=g(x_i)\delta_{ij}.$$

Doing the same with a differential operator of the form $(d/dx)\xi(x)\pi_i(d/dx)\xi(x)\pi_j$, we get

$$\xi'(x_i)^2\delta_{ij}+\xi(x_i)\xi'(x_i)\sqrt{W_i}\pi_j'(x_i)$$

$$+\xi(x_j)\xi'(x_j)\sqrt{W_j}\pi_i'(x_j)+\sum_k \xi(x_k)^2\pi_i'(x_k)\pi_j'(x_k). \tag{B1}$$

In practice, we set

$$\xi(x)=r=\frac{r_0}{2}(1+x) \tag{B2}$$

in order to ensure the vanishing boundary condition at $r=0$. It is straightforward to evaluate $(d/dx)\pi_i(x_k)$ with high precision by way of $(d/dx)\phi_n(x_i)$ using $\phi_n(x_i)$ and $\phi_{n-1}(x_i)$. So once $\phi_n(x_i)$ is tabulated for all the pairs of (n,i), we have the matrix elements of the differential operator with respect to DVR to the precision afforded by the Gaussian quadrature. However, the computational burden in this case is not lessened significantly despite DVR on account of the triple summation in the last term of Eq. (B1).

APPENDIX C: SIEGERT REPRESENTATION OF THE GREEN'S FUNCTION

The Green's function is formally given by $(\mathcal{K}-\kappa\rho)^{-1}$, whose spectral representation is

$$G=\sum_n \frac{S_n\langle S_n^T|\rho|S_n\rangle^{-1}S_n^T}{\kappa_n-\kappa}. \tag{C1}$$

Substituting the block-matrix representations of $\mathcal{K}$ and ρ, and decomposing G into

$$G=\begin{pmatrix} G_{11} & G_{12} \\ G_{21} & G_{22}\end{pmatrix},$$

we can formally identify $G_{11}=\frac{1}{2}(H-E)^{-1}$ [where $H=i\hbar(\partial/\partial t)$ as defined in Eq. (1)] by simply considering the inverse of

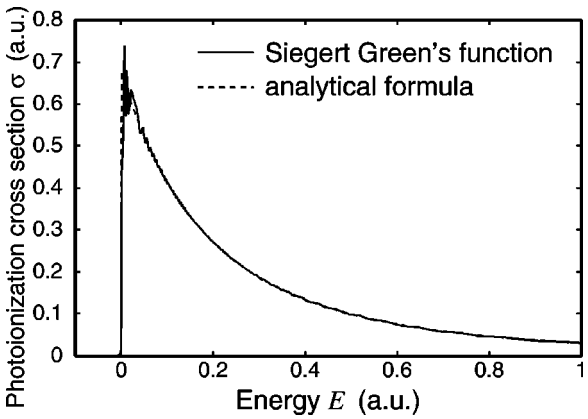

FIG. 8. Photoionization cross sections of hydrogen. The solid line by the Siegert Green's function. The broken line by the well-known analytical formula (see text).

$$\mathcal{K}-\kappa\rho=\begin{pmatrix} 2\mathcal{H}-\kappa\mathcal{B} & \kappa \\ \kappa & -\mathbf{1}\end{pmatrix}.$$

However, we also need to identify the proper branches of energy E in order to separate the retarded and advanced Green's functions. Meanwhile, the block of Eq. (C1) corresponding to G_{11} is

$$\mathcal{G}^{(1)}=\sum_{n=1}^{2N}\frac{c^{(n)}c^{(n)T}}{2\kappa_n(\kappa_n-\kappa)}.$$

The form corresponding to the other branch of κ derives from $(\mathcal{K}+\kappa\rho)^{-1}$, and is given by

$$\mathcal{G}^{(2)}=\sum_{n=1}^{2N}\frac{c^{(n)}c^{(n)T}}{2\kappa_n(\kappa_n+\kappa)}.$$

The sum $\mathcal{G}^{(1)}+\mathcal{G}^{(2)}$ reduces to

$$\sum_{n=1}^{2N}\frac{c^{(n)}c^{(n)T}}{E_n-E},$$

which upon Laplace transform is readily seen to consist of the retarded and advanced Green's functions. Separating κ_n and κ_n^*, which are both poles, we get the retarded and advanced Green's functions, respectively,

$$G^{(+)}=\sum_{n=1}^{N}\frac{c^{(n)}c^{(n)T}}{E_n-E}\quad(\mathrm{Im}E_n>0), \tag{C2}$$

$$G^{(-)}=\sum_{n=1}^{N}\frac{c^{(n)}c^{(n)T}}{E_n-E}\quad(\mathrm{Im}E_n<0), \tag{C3}$$

where the sum now runs over N eigenvalues of E_n. In evoking time propagation with respect to the Siegert pseudostates, we must keep to the retarded Green's function such that $\mathrm{Im}E_n<0$.

To end this appendix, we give a simple illustrative demonstration of the advanced Green's function based on the Siegert pseudostates. It is the photoionization cross section of hydrogen given by

$$\sigma = \frac{4\pi}{c}\hbar\omega\,\mathrm{Im}\sum_n \frac{\langle 0|d|c^{(n)}\rangle\langle c^{(n)T}|d|0\rangle}{E_n - E},$$

where d is the dipole operator and $|0\rangle$ is the initial ground state, which is volume-normalized to unity. We compare in Fig. 8 the photoionization cross sections calculated according to the above formula with those of the analytical one [15]. The agreement is good considering the rather wide energy spectrum covered by 150 basis functions. The box size r_0 is 400 a.u. An artifact due to the use of the finite basis set is visible near threshold in the form of sawtoothed structures.

[1] S. Yoshida, S. Watanabe, C.O. Reinhold, and J. Burgdörfer, Phys. Rev. A **60**, 1113 (1999).

[2] Oleg I. Tolstikhin, Valentin N. Ostrovsky, and Hiroki Nakamura, Phys. Rev. A **58**, 2077 (1998).

[3] B. Schneider, Phys. Rev. A **24**, 1 (1981).

[4] M.T. Frey, F.B. Dunning, C.O. Reinhold, S. Yoshida, and J. Burgdörfer, Phys. Rev. A **59**, 1434 (1999), and references therein.

[5] C.O. Reinhold, J. Burgdörfer, M.T. Frey, and F.B. Dunning, Phys. Rev. Lett. **79**, 5226 (1997); S. Yoshida, C.O. Reinhold, P. Kristöfel, J. Burgdörfer, S. Watanabe, and F.B. Dunning, Phys. Rev. A **59**, R4121 (1999).

[6] See, for instance, Bruce W. Shore, *The Theory of Coherent Atomic Excitation* by (John Wiley & Sons, New York, 1990), Vol. 2, pp. 938–949.

[7] S.A. Gardiner, D. Jaksch, R. Dum, J.I. Cirac, and P. Zoller, Phys. Rev. A **62**, 023612 (2000).

[8] R. Z. Sagdeev, D. A. Usikov, and G. M. Zaslavsky, *Nonlinear Physics: From the Pendulum to Turbulence and Chaos* (Harwood Academic Publishers, New York, 1988), pp. 513–528.

[9] This type of adiabatic diagonalization is actually employed in a similar context of atomic diamagnetism. See, for instance, S. Watanabe, Y. Hosoda, and H. Komine, Phys. Rev. A **46**, 2693 (1992).

[10] J.C. Light, I.P. Hamilton, and J.V. Lill, J. Chem. Phys. **82**, 1400 (1985); S.E. Choi and J.C. Light, *ibid.* **90**, 2593 (1989).

[11] See, for instance, William H. Press, Saul A. Teukolsky, William T. Vetterling, and Brian P. Flannery, *Numerical Recipes* (Cambridge University Press, New York, 1992).

[12] S. Tanabe and S. Watanabe (unpublished).

[13] C. Schwartz, J. Math. Phys. **26**, 411 (1985).

[14] J.-M. Launay (private communications).

[15] For instance, U. Fano and A. R. P. Rau, *Atomic Collisions and Spectra* (Academic Press, New York, 1986), p. 40.